



HAL
open science

Pith location tool and wood diameter estimation: Validity and limits tested on seven taxa to approach the length of the missing radius on archaeological wood and charcoal fragments

Alexa Dufraisse, Jérémie Bardin, Llorenç Picornell-Gelabert, Sylvie Coubray,
Maria-Soledad Garcia-Martinez, Michel Lemoine, Silvia Vila Moreiras

► **To cite this version:**

Alexa Dufraisse, Jérémie Bardin, Llorenç Picornell-Gelabert, Sylvie Coubray, Maria-Soledad Garcia-Martinez, et al.. Pith location tool and wood diameter estimation: Validity and limits tested on seven taxa to approach the length of the missing radius on archaeological wood and charcoal fragments. *Journal of Archaeological Science: Reports*, Elsevier, 2020, 29, pp.102166. 10.1016/j.jasrep.2019.102166 . mnhn-03008213

HAL Id: mnhn-03008213

<https://hal-mnhn.archives-ouvertes.fr/mnhn-03008213>

Submitted on 16 Nov 2020

HAL is a multi-disciplinary open access archive for the deposit and dissemination of scientific research documents, whether they are published or not. The documents may come from teaching and research institutions in France or abroad, or from public or private research centers.

L'archive ouverte pluridisciplinaire **HAL**, est destinée au dépôt et à la diffusion de documents scientifiques de niveau recherche, publiés ou non, émanant des établissements d'enseignement et de recherche français ou étrangers, des laboratoires publics ou privés.

1 **Pith location tool and wood diameter estimation: validity and limits tested on seven taxa**
2 **to approach the length of the missing radius on archaeological wood and charcoal**
3 **fragments.**

4
5
6
7 DUFRAISSE, Alexa¹

8 BARDIN, Jérémie²

9 PICORNELL-GELABERT, Llorenç³

10 COUBRAY, Sylvie^{1,4}

11 GARCIA-MARTINEZ, Maria Soledad^{1,5}

12 LEMOINE, Michel¹

13 VILA MOREIRAS, Silvia^{1,6}

14
15 1. CNRS/ MNHN, UMR 7209 Archéozoologie, Archéobotanique: Sociétés, Pratiques et
16 Environnements, Sorbonne Université, CP56, 55 rue Buffon, 75005 Paris, France.

17 alexa.dufraisse@mnhn.fr. Corresponding author

18 2. Sorbonne Université, MNHN, CNRS, Centre de Recherche en Paléontologie - Paris (CR2P),
19 4 Place Jussieu, 75005 Paris, France.

20 3. ArqueoUIB Research Group. Department of Historical Sciences and Theory of Arts.
21 University of the Balearic Islands. Carretera de Valldemossa KM 7, 5, 07122, Palma, Balearic
22 Islands, Spain.

23 4. INRAP Centre-Ile-de-France, 41 rue Delizy, 93690 Pantin cedex

24 5. Departamento de Prehistoria, Arqueología, Historia Antigua, Historia Medieval y Ciencias
25 y Técnicas Historiográficas, Facultad de Letras, Universidad de Murcia. C/ Santo Cristo, 1.
26 30001-Murcia.

27 6. Dpt. de Història. Universitat de Lleida 25003 Lleida, Spain.

28
29
30 **Abstract**

31 The study of timber wood and wood charcoal fragments from archaeological sites (aka
32 anthracology) constitutes a relevant archaeobotanical field of research for both landscape
33 reconstruction and the study of past people-woodlands interactions. Regarding this second
34 research field, variables other than taxa are known to be a key to the social organization of
35 woodland management. In this sense, wood diameter constitutes a core factor of fire
36 management, fuel provisioning and both firewood and timber procurement. These wood uses
37 are most commonly represented in the archaeological record by charcoal fragments (both
38 dispersed in the sediment and/or concentrated in fire structures) due to the fact the wood
39 experiences both mass loss and fragmentation during carbonization. So the original form of the
40 wood used (trunk, branch, twig) is no longer recognizable. Different pith-location tools (PLT)
41 have been proposed previously in order to virtually locate the charcoal fragment in relation to
42 the central part of the stem or trunk (pith) where the used wood originally came from. Among
43 them, PLTs based on trigonometry are proven to be the most reliable, but have not yet been

44 extensively tested on referential datasets in order to establish reliable analysis of the accuracy
45 of the measurement of the missing radius, margins of error and correction factors. In this study
46 we present an experimental referential dataset for 7 different taxa, both angiosperms and
47 gymnosperms. The first aim was to move forward on the establishment of the trigonometric
48 tool by testing if it is also suitable and valid for all the woody species producing tree rings. The
49 second purpose was to provide a ready-to-use tool to estimate the missing radius with an
50 interval of confidence. Lastly we also tested the effect of the carbonization on two taxa.
51 According to the results obtained, a measuring protocol, correction factors and guidelines to
52 interpret the subsequent results are established. In addition, an R function is now available to
53 estimate the real radius from the calculated one with PLTs.

54

55 **Keywords:** wood pith location; referential datasets; software; dendro-anthracology; wood
56 diameter estimation; firewood and timber exploitation

57

58

59 **Introduction**

60

61 Wood diameter constitutes a social selection criterion as relevant as species, whether to manage
62 a fire according to the uses of the hearth or to select timber for construction or woodworking as
63 shown by diverse ethnoarchaeological studies (Zapata Peña et al., 2003; Dufraisse et al., 2007;
64 Picornell-Gelabert et al., 2011). The carbonized and fragmented residues of this use of wood as
65 firewood or timber are most often preserved in the archaeological record (charcoal fragments
66 dispersed on the sediments and/or concentrated in fire structures, such as hearth and ovens).
67 Wood experiments both mass loss and fragmentation during carbonization, so the original form
68 of the wood used (trunk, branch, twig) is no longer recognizable. This fact makes it difficult to
69 archaeologically evaluate the role of the wood diameter as a selective criteria of wood uses and
70 woodlands management by past human societies.

71 In recent years, new measurement techniques have been developed in order to estimate the
72 diameter of the wood from which the archaeological charcoal fragments originates. One of the
73 main research fields in this sense is the establishment of reliable techniques to measure the
74 distance between the preserved archaeological charcoal fragment and the pith of the
75 trunk/branch where the fragment comes from. This measurement technique consists of virtually
76 positioning a charcoal fragment in relation to the central part of the stem or trunk (pith), which
77 is missing in most of the cases (pith-location tool, PLT). This measurement constitutes a

78 necessary first step to latter estimate the original diameter of the wood exploited in the past
79 (Dufraisse and Garcia-Martinez, 2011).

80 Different “naked-eye” methods guided by a printed graduated target and based on tree-ring
81 boundary’ morphology (ring curvature) were proposed to estimate the length of the missing
82 radius (Applequist, 1958; Willerding, 1971; Lundström-Baudais, 1986; Ludemann and Nelle,
83 2002; Rozas, 2003; Dufraisse, 2005; Marguerie and Hunot 2007).

84 Later on, experimental research was set up to evaluate two techniques of measurement using
85 image-analysis software. The “circle tool technique” is one of them, initially proposed by J.
86 Chrzavzez (2006) and based on the curvature of tree-ring boundaries. Another tool tested, the
87 “trigonometric tool”, is based on the measurement of angles and distance between ligneous
88 rays, proposed by A. Dufraisse and developed together with S. Paradis-Grenouillet and M.S.
89 Garcia-Martinez (Paradis-Grenouillet et al., 2013; Dufraisse and Garcia-Martinez, 2011). These
90 studies were developed on different taxa, *Quercus petraea*, *Pinus halepensis* and *Fagus*
91 *sylvatica*. They showed that measurements of the radius of curvature based only on the
92 curvature of the tree-ring boundaries must be avoided due to the fact that calculated missing
93 radius did not correspond to the real radius.

94

95 On the contrary, the estimation of the missing radius on the 3 taxa tested (*Quercus petraea*,
96 *Fagus sylvatica* and *Pinus halpensis*) with the trigonometric tool (angle and distance between
97 ligneous rays) in a right-angled triangle provides relevant results:

98 *i*) Strong correlation exists between the exact value of the length of the missing radius (real
99 radius, RR) and its measurement (calculated radius, CR);

100 *ii*) Other trigonometric techniques, such as Thales’ theorem and trigonometry in an isosceles
101 triangle, provide similar results (Paradis-Grenouillet et al., 2013).

102

103 Building on this previous research, the aim of this study is to move forward on the establishment
104 of the trigonometric tool by testing if it is also suitable and valid for all the woody species
105 producing tree rings and to provide a ready-to-use tool to estimate the missing radius with an
106 interval of confidence. To do so we establish an empirical reference dataset for seven different
107 taxa with different wood anatomy (both conifers and angiosperms) and commonly identified in
108 archaeological charcoal spectra in Europe. We later compare the relative errors between species
109 according to 1) the angle and the distance between the two ligneous rays 2) and the diameters.

110

111 As the Pith Location Tool (PLT) is mainly applied to wood charcoal fragments, we also
112 investigate the effect of the carbonization, which induces deformation (distortion of shape and
113 shrinkage), on the efficiency in evaluating the missing radius with the PLTs.

114
115

116 **Materials and methods**

117 The referential dataset was developed in the framework of the DENDRAC project
118 “Development of DENDRometrical tools used in anthrACology: study of the interactions
119 between man, resources and environments” funded by the French National Agency of Research
120 (<http://dendrac.mnhn.fr/>). This program follows key experimental principles to allow relevant
121 subsequent comparisons of the data obtained, mainly the use of common protocols for all the
122 different taxa and a restricted number of operators.

123

124 *Measurement tools and materials*

125

126 All the measurements were performed using the NIS Element image-analysis software
127 developed by Nikon. The NIS Elements software was associated to a Nikon camera assembled
128 to a multizoom microscopes (Nikon AZ100) with objectives covering a diverse range of
129 magnifications (from x5 to x400) and to a binocular stereo microscope (Nikon SMZ 745, x6 to
130 x50). Different PLTs based on trigonometric principles were tested. They are all based on the
131 acquisition of two measures at the same ring boundary: 1) the angle between two ligneous rays
132 and 2) the distance between the same two ligneous rays. These measurements allow estimating
133 the length of the missing radius (this is, the distance between the ring boundary measured and
134 the missing pith).

135

136 The first PLT is a manual one, based on the trigonometry in a right-angled triangle and
137 involving 12 landmarks fixed by using the NIS element software. The measurements were
138 carried out under a binocular stereoscope with x10 magnification and a measurement field of
139 L0,84 cm x h0,63 cm, compatible with small fragments often found in archaeological charcoal
140 assemblages.

141

142 The second PLT is a semi-automatic method based on 4 landmarks, which is less time-
143 consuming and more adapted to a routine use. Based on the trigonometry in an isosceles
144 triangle, it was tested under the multizoom microscope with an objective of x0.5 magnification

145 and digital zoom (e.g. measurement field dimensions with the lowest magnification: L 2,2 cm
146 x h1,7 cm).

147

148 The two PLTs (manual and semi-automatic) were tested on perfect targets printed on white
149 paper. The referential based on fresh and carbonized wood slices was realised with the manual
150 PLT and completed with the semi-automatic PLT.

151

152 - Perfect target

153 The PLTs were first calibrated on perfect targets with a range of radius between 0.5 cm and
154 17.5 cm (i.e. range of diameter : 1;2;3;5;10;12;15;18;20;25;30;35 cm) and angles between 2
155 and 70°.

156 For each method of measurement (manual and semi-automatic), from 25 to 30 measures were
157 carried out according to radius and angles, e.g. 1320 measures / method and 2640 measurements
158 in total (Table 1). In some cases (see * in Table 1), measurements could not have be taken due
159 to either the dimension of the measurement field or printing problems with the target especially
160 between 0.5 and 1 cm of radius and small angles (2° and 4°).

161

162 - Fresh wood

163 Seven taxa with different anatomical characteristics (Angiospermae vs Gymnospermae,
164 presence of uniseriate and/or multiseriate rays, ring porous/diffuse wood, etc.) were studied:
165 Gymnosperm: *Pinus halepensis* (uniseriate rays); ring porous Angiosperms: *Quercus petraea*
166 (uni- and multiseriate rays), *Castanea sativa* (uniseriate rays), *Fraxinus excelsior* (2-3 seriate
167 rays), *Ulmus minor* (3-5 seriate rays); diffuse porous Angiosperms: *Fagus sylvatica*
168 (multiseriate), *Prunus avium* (3-5 seriate rays). As far as it was possible, from one to six wood
169 slices from different trees coming from different locations were analysed for every taxon to
170 record a maximum of variability (excepted for *Ulmus*, *Prunus* and *Castanea*). Measurements
171 were performed on fresh wood slices after a fine sanding of the surface. A total of 4164
172 measures were carried out (see the total number of measurements in Table 2).

173

174 - Carbonized wood

175 In order to evaluate the PLT on carbonized wood slices, we measured before and after
176 carbonization two of the studied taxa: *Pinus halepensis* and *Fagus sylvatica* (Table 2). Two
177 wood slices for *Pinus* (R1, R2) and one for *Fagus* (R13) were carbonized in a muffle furnace
178 at 300°C during two hours according to its thickness. The measured shrinkage fluctuates from

179 14.7% (slice R2, 14,5 x 13 cm) to 15.38% (slice R1, 16,5x 16,4 cm) and is about 20% on *Fagus*
180 *sylvatica* (R13). In total, 720 measures were carried out on this carbonized material (Table 2).

181

182 *Data Treatment*

183

184 The PLT we provide consists in producing an estimation of the real radius (RR) given the
185 calculated radius (CR). For each measure, we registered the real radius (RR), the angle and the
186 distance between the two rays, and the calculated radius by using the trigonometric tool (CR).

187 The relative error (RE) was calculated following the equation: $RE = (CR - RR) * 100 / RR$. Some
188 values of RE are negative due to possible underestimations of CR. In order to have a comparable
189 measure of error (i.e. both negative and positive), we used the Absolute Relative Error: $ARE =$
190 $(|CR - RR|) * 100 / RR$.

191

192 While most of the observations follow a straight regression line, for small angles, CR and thus
193 ER show obvious outliers. We tried several methods to identify and remove them in order to
194 provide the user a practical minimum angle (see SM1). Unfortunately, none of these methods
195 allowed us to identify a clear angle limit from which all observations could be included. As we
196 want to perform the regressions on every observations starting from a given angle to include
197 the whole variation of the selected range, we chose 2° as the lower limit, a solution which is
198 reproducible on archaeological charcoal assemblages.

199

200 In order to understand the relation between RR and CR, we use our dataset as a training sample
201 in order to establish models suited to estimate the RR on archaeological wood / charcoal
202 fragments based from the CR by using the provided PLT. An eye-check on a bivariate
203 representation of RR over CR (see Fig. 3 in Results) strongly suggests that the relationship
204 between these two variables is linear. We therefore try to model this relationship with a linear
205 model with RR as the response variable and CR as the explanatory variable (*reg*). The variance
206 of RR increases over the range of CR. To take this into account, we performed a weighted
207 regression with the weights of each observation being $1/CR$ (*wreg*). Secondly, we noticed that
208 the relationship between RR and CR may be piecewise, with a potential important decrease of
209 the slope for highest values of CR (see Fig. 4 in Results). To investigate this issue, we fit a
210 regression model for each species with broken line relationships (*swreg* = segmented weight
211 regression model) using the R package *segmented* (Muggeo, 2008). This model can be viewed
212 as a linear regression from which we allow the relationships between CR and RR (i.e the slope)

213 to change on each side of a breakpoint represented by the parameter α . Using such a model is
214 of prime importance as the relationship seems stronger for low values of CR. This allows us to
215 test precisely each part of the relationship and to locate on which of those part the prediction
216 are the best. AIC (Akaike, 1973) allows finding the adequate balance between the goodness of
217 fit and the number of parameters. We use it to select the best model for each species (i.e. reg,
218 wreg, swreg; Table 3).

219
220

221 To investigate the effect of carbonization on the relationship between CR and RR, we add to
222 the model swreg an additional discrete variable representing the carbonization (here after called
223 *swregCarb*). We use the approach proposed by Muggeo (2008) to split the values of the
224 explanatory variable (i.e. CR) for the different levels of the factor (i.e. carbonized or not).

225

226 **Results**

227 *Comparison of manual and semi-automatic PLTs on perfect target*

228

229 The analysis of the manual PLT on perfect target is based on 1320 measurements. The mean of
230 the Absolute Relative Error (ARE) and its standard error is $3.52\% \pm 0.48$. The correlation of
231 the exact and the approximated value of the radius is 0.9953078 (method = Spearman, p-value
232 $< 2.2e-16$).

233 The test of the semi-automatic PLT is also based on 1320 measurements. The mean of ARE
234 and its standard error is $2.44\% \pm 0.3$. The correlation of the exact radius and the approximated
235 radius is 0.9958947 (method = Spearman, p-value $< 2.2e-16$).

236 A Wilcoxon-Mann-Whitney test between RE from the manual and the semi-automatic PLT
237 indicates a significantly different median. However, the differences are very fine as shown by
238 Figure 1. Indeed, the manual PLT has a slightly negative ER when semi-automatic PLT is
239 centred on zero. Then, the semi-automatic PLT works slightly better than the manual PLT.

240

241 *Establishment of exclusive criteria*

242

243

244 The analysis of the distribution of the Relative Error (RE) on perfect targets, according to angle
245 and distance, indicates that the distribution of RE decrease obviously from angles bigger than
246 10° . The biggest RE is reached for the smallest angle (2° , ARE = 5.27%, sd= 4.39%) (Fig. 2).
247 The analysis of RE values according to RR indicates that there is no correlation between these
248 two parameters (Pearson correlation coefficient = 0.009, p-value = 0.5).

249

250 Thus, exclusive criteria to avoid inexact measurements using the PLT on archaeological
251 charcoal fragments have been established according to the analysis of the referential dataset.

252 Indeed, for all taxa together (fresh wood), and all angles and distances included, the mean of
253 the ARE and its standard deviation are 0.511 ± 5.47 .

254 The analysis of the RE according to distance and angle indicates that the most important RE
255 concerns angle below 2° (Fig. 2, SM2). Most often, these small angles correspond to small
256 distances between rays, less than 2 mm. Integrating these exclusive criteria, the mean of the
257 ARE and its standard deviation are 0.25 ± 0.24 . The correlation between the exact values of
258 radius and its approximate values is 0.8832283 (method = Spearman, p-value $< 2.2e-16$). The
259 following analyses presented include the exclusive criteria.

260

261

262 *Comparison between taxa (fresh wood) and modeling of the relation between RR and CR*

263

264

265 The bivariate representation of RR over CR (Fig.3) from data measured on fresh wood strongly
266 suggests that the relationship between these two variables is linear. However, the variance of
267 RR increases over the range of CR.

268 A comparison of the results obtained with the referential analysis was performed in order to
269 compare the results of the PLT on the different taxa and to model the relation between the RR
270 and the CR (Table 4, data treatment). Thus, a regression model for each species with broken
271 line relationships was performed (Fig. 4, Table 4).

272

273 The first slopes (lowest CR) are very similar between taxa excepted for *Pinus halepensis*.
274 Indeed, very low CR values corresponding to a wide range of RR values are to be noted without
275 explanation (Fig. 3, *Pinus halepensis*).

276 Thus, the smallest breakpoint concerns *Pinus halepensis* with a CR of 4.071 cm that means
277 about 8 cm of diameter. Below this breakpoint, the correlation between CR and RR is very
278 strong while above 4 cm, the estimation of RR from CR is no more reliable, characterized by a
279 nearly flat regression line.

280 The swreg model indicates also a low breakpoint for *Quercus petraea* as for *Pinus*. However,
281 after this breakpoint, CR is still correlated with RR even if the interval of confidence is large.

282

283 At the opposite, the highest breakpoint corresponds to *Prunus avium* with a CR = 9.833 cm that
284 means about 20 cm of diameter. In other words the correlation between CR and RR is very
285 strong for diameters less than 20 cm while the estimation of RR for largest diameter is no more
286 reliable, characterized by a downward slope. *Fagus sylvatica* presents similar behavior.

287

288 Lastly, *Ulmus minor*, *Fraxinus excelsior* and *Castanea sativa* are between these two groups
289 with a breakpoint at CR = 5.475, CR = 6.958 and CR = 6.043, respectively. Before the
290 breakpoint, the correlation between RR and CR is very strong. After it, the correlation is less
291 accurate but still reliable despite a large interval confidence (the signal is preserved).

292

293 *Effects of carbonization*

294 In order to evaluate the efficiency of the PLTs on carbonized wood, we repeated the same
295 protocols on carbonized slices for *Pinus halepensis* and *Fagus sylvatica*. (Fig. 5, Table 5). To
296 carry out this comparative analysis, we considered only measurements from fresh wood slices
297 that were charred (i.e. R1 and R2 for *Pinus*, and R13 for *Fagus*).

298

299 The effect of carbonization is almost negligible on *Pinus sylvestris*. The breakpoint value is
300 small before carbonization (CR = 4.168 cm). It slightly increases after carbonization (CR =
301 4.91). In fact, the above-mentioned marginal measures are no longer recorded on carbonized
302 slices, which is the reason why the slope 1 of carbonized wood is slightly less inclined and the
303 breakpoint slightly higher. After carbonization, it is interesting to note that the slope 2 is slightly
304 less flat.

305 On the contrary, the carbonization induces significant changes in the RR estimation for *Fagus*
306 *sylvatica* whose breakpoint value was high before carbonization (CR = 7.717 cm) and smaller
307 after carbonization (CR = 4.717 cm). Nevertheless, the slope 1 and the slope 2 before and after
308 carbonization are very similar. That means the signal is preserved.

309

310 **Interpretation and Discussion**

311 *PLTs on perfect targets*

312 A manual technique with 12 landmarks and a semi-automatic technique with 4 landmarks (less
313 time consuming and more suitable for a routine use) using the trigonometric principle were
314 compared on perfect target printed on white paper. The 1320x2 measures developed show quite
315 comparable results even if the statistical test indicates a median significantly different. A
316 previous study showed that Thales' theorem, trigonometry in a right-angled triangle, and

317 trigonometry in an isosceles triangle provide relevant and similar results. They are just more or
318 less adapted to the software used (Paradis-Grenouillet et al., 2013). Two reasons can be given
319 to explain why the semi-automatic PLT works slightly better than the manual one. The first one
320 is the observation equipment. The manual PLT was associated to a binocular stereoscope that
321 is not recommended in morphometry. The second one is the smaller number of landmarks for
322 the semi-automatic PLT (4 landmarks instead of 12 for the manual PLT). Indeed, the recorded
323 relative errors on perfect target are related to handling, i.e. to the operator. Then, the smaller
324 the number of landmarks is, the less the margins of error are important.

325

326 *PLTs on fresh wood*

327 The values of relative errors on fresh wood slices are significantly higher than on perfect targets.
328 This means that the larger relative errors on fresh wood are related to the anatomy of the wood,
329 as the RE linked to the operator is marginal. It is impossible to escape this margin of uncertainty,
330 which is intrinsic to any living phenomenon, as each characteristic of an organism results from
331 the interaction between its genome and the environment, which is itself greatly variable.

332 In order to limit the margins of error, an exclusive criterion could be set up for the
333 archaeological application of the PLT: avoid angles $< 2^\circ$. In addition, whichever the taxon, RE
334 values increase significantly in relation to the distance from the pith. Observations of the wood
335 slices suggest that this is due to the fact that new ligneous rays are inserted during growth of
336 the stem, the latter not necessarily converging at the level of the pith. In addition, when tension
337 wood occurs during growth, the direction of the rays can change to adapt to the new wood
338 morphology. Also, the observation scale, often limited to a camera field about 1 cm², does not
339 allow to assess local deformations or wood rays which can also be a source of error (Fig. 6).

340

341 *Comparison between taxa*

342 The variance of RR estimations on fresh wood increases for all taxa over the range of CR. The
343 segmented weighted regression model allows comparing different taxa. The slope 1, before the
344 breakpoint, is very similar for all taxa excepted for *Pinus halepensis* due to marginal values.

345 Then, the model indicates similarities between taxa. For example, *Fagus* and *Prunus*, whose
346 anatomy is very close, are characterized by a high breakpoint (about 10 cm in radius). However,
347 after this breakpoint, the signal is lost (see slope 2). These two species are diffuse porous wood
348 with multiseriate rays. Thus, deformation linked to large vessels in earlywood, as it can be seen
349 in porous wood, is probably limited.

350

351 Other similarities can be observed between *Fraxinus*, *Castanea* and *Ulmus*, whose anatomy is
352 also close. Their breakpoint ranges from 5.4 cm to 6.9 cm. The signal is well preserved after it
353 for *Fraxinus*, which is less obvious for *Castanea* and *Ulmus* (see slope 2).

354 Another group is formed by *Pinus* and *Quercus*. They are both characterized by a small
355 breakpoint (about 4 cm in radius). Nevertheless, the signal is better preserved after this
356 breakpoint for *Quercus* than for *Pinus*, even if their anatomy is significantly different.

357

358 According to these results, wood anatomy, especially the ligneous rays and probably their
359 formation, may be an explanation of such variations. However, surprisingly, our understanding
360 of how wood develops, especially wood rays, is far from complete (for a review, see Lev-
361 Yadun and Aloni, 1995). Short radial initials (cells in the cambium) give rise to rays that are
362 essential to the translocation of nutrients between phloem and xylem. As for other wood
363 elements such as vessels, the cellular and molecular processes are controlled by a wide variety
364 of factors both exogenous (photoperiod and temperature) and endogenous (phytohormones) and
365 by interaction between them (Plomion et al., 2001). According to Lev-Yadun and Aloni
366 (1995), a basic aspect of maturation in woody plants is the normal gradual increase in ray size
367 with age, with distance from the pith, and with distance from the young leaves. However, the
368 increase in size and number of rays is not necessarily dependent on the distance between rays.
369 The greater number of rays generally observed in branches, as compared with the stem, no
370 doubt correlates with the reduced width of the rings and the associated reduction in caliber of
371 the tracheids. In *Fraxinus excelsior* and *Castanea sativa* there were more rays per unit area in
372 the wood with wide growth rings than there were in the slower-growth wood. Concerning *Pinus*
373 *halepensis*, there is no clear, general conclusion that the rate of cambial activity determines the
374 number of rays. Lev-Yadun and Aloni (1995) concludes that the rate of cambial activity is not
375 the only regulating mechanism of ray characteristics, and another explanation for the regulation
376 of ray formation during cambial activity is needed.

377

378 *Effect of carbonization*

379 The results indicate that the effect of the carbonization is different depending on the two taxa.
380 It is almost negligible on *Pinus*, while on *Fagus* we can observe an obvious decrease of the
381 breakpoint. The slope 1 is very similar before and after carbonization for the both taxa. After
382 the breakpoint, the slope 2 indicates that the signal is not well preserved. However, the
383 reference data is still limited and have to be completed. Xue et al. (2018) analysed the effect of

384 wood rays on the shrinkage of wood during the drying process. The wood is characterized by
385 an anisotropic shrinkage (as well as during the carbonization): the longitudinal shrinkage from
386 the green to the dried condition (and during carbonization) is the smallest and the tangential
387 shrinkage is usually 1.5 to 2.5 times that of radial shrinkage. Their experiments indicate that
388 the larger the rays, the greater the shrinkage of fibers. In addition, fiber shrinkage is clearly
389 dependent on the distance from the wood rays. If this study concerns the wood drying process,
390 it could be assumed that this same process may occur during the carbonization with greater
391 effects. The most important decreasing of the breakpoint value observed on *Fagus* can thus be
392 explained by the numerous and multiseriate rays.

393

394 *Measurement protocol*

395

396 Considering the results of this referential study, a measurement protocol can be established in
397 order to provide a ready-to-use PLT to estimate the missing radius with an interval of
398 confidence. According to the results, the semi-automatic PLT using a multizoom microscope is
399 preferred, as it reduces the margins of errors (and measures) and is less time-consuming.
400 Accordingly, the following protocol is established in order to obtain reliable estimations of the
401 charcoal-pith distance for archaeological wood and charcoal fragments and to estimate the
402 original diameter of the wood used:

403

404 1- Each charcoal fragment to measure have to present at least one preserved ring (this is two
405 ring boundaries) in a transverse section of at least 2 mm length is needed in order to provide a
406 reliable assemblage to be measured. A limit inherent to the size of archaeological charcoal,
407 especially for fragments smaller than 4 mm, is noticeable. This limit is directly related to the
408 minimum angle that must be exceeded to obtain a reliable measurement (2°). Thus, the
409 maximum missing radius that can be measured on transversal section smaller than 4mm*4 mm
410 is 11.5 cm (23 cm diameter) (Nocus, 2014).

411

412 2- Orientate each wood/charcoal fragment under the multizoom microscope in order to verify
413 that the rays are not divergent. Do not measure fragments presenting deformed wood anatomy.
414 As far as possible, take measurements on the last ring boundary preserved. Eliminate the
415 measurements with angles $<2^\circ$.

416

417 3- Repeat 3 to 5 times the measure on the same ring boundary and with different rays. Discard
418 the two extreme values (largest and smallest measurements of the missing radius) and calculate
419 a mean value with the three remaining measures.

420

421 4- An R function and the swreg model with a user guide can be downloaded on the DENDRAC
422 website in the section Dendro-anthracological tools
423 (<https://dendrac.mnhn.fr/spip.php?rubrique71>). The function allows to obtain, from the CR, a
424 RR with margins of error following the model presented in the paper. The result can be
425 improved considering each taxon independently and/or the state of carbonization. If the taxon
426 are not referenced in the database, the estimation of RR is given taking into account all the taxa.

427

428 5- If the analysed material is carbonized, correct the shrinkage due to carbonization. At the state
429 of the art, we assume a mean of 20% in open domestic fireplace. The value can reach 40% in
430 charcoal kilns. A more precise reference was conducted on *Quercus* and *Castanea* at different
431 temperatures and taking into account sapwood and heartwood (Paradis-Grenouillet and
432 Dufraisse, 2018)

433

434 6- (optional) Double the CR final value and locate it into one of the diameter classes proposed
435 for angiosperms and gymnosperms (this is the actual value that will allow discussing the
436 composition of the assemblage in relation to diameter). Considering the accuracy of the RR
437 estimated and the standards used in dendrometrical plans by foresters (Gaudin, 1996; Deleuze
438 et al., 2014), the values of estimated RR can be ordered into diameter classes as following for
439 Angiospermae: [0-2] cm, [2-4] cm, [4-7] cm, [7-10] cm, [10-20] and >20 cm; and as following
440 for Gymnospermae: [0-2] cm, [2-4] cm, [4-7] cm, [7-10] cm, [10-14] cm, [14-20] cm and >20
441 cm (Dufraisse et al., 2018). However, taking into account the segmented weighted regression
442 models, data must be interpreted with caution between [10-14] cm, [14-20] cm. It is also
443 important to note that referential studies for other Gymnospermae should be considered in order
444 to strength the model for these taxa.

445

446 *Contributions of the use of the trigonometric PLT on archaeological charcoal assemblages.*

447 The PLT has been tested on archaeological charcoal analysis to approach wood management
448 strategies on different contexts. García-Martínez and Dufraisse (2012) analysed charcoal
449 fragments at the Argaric Bronze Age site of Barranco de la Viuda, South-Eastern Iberia. In this
450 case, charcoal-pith distance for diameter restitution has been performed on Aleppo pine (*Pinus*

451 *halepensis*) charcoal fragments from three different assemblages. Small diameters (>10 cm,
452 mainly 2-5 cm) were exploited to provide firewood for different dwelling and craft activities
453 performed at the site. The occurrence of saproxylophagous in some of the branches suggested
454 that firewood provisioning at the site focused on the gathering of Aleppo pine dead branches.

455

456 Aleppo pine charcoal fragments have also been analysed in Late Bronze Age and Iron Age sites
457 of Mallorca (Balearic Islands, Western Mediterranean, Picornell-Gelabert and Dufraisse 2018).
458 Assemblages of dispersed charcoal fragments from two different sites abandoned after fire
459 events were analyzed in order to suggest the original use of pinewood before the firing of the
460 buildings. At Ses Païsses site the occurrence of diameters >7 cm was minor, while at Son Fornés
461 site the occurrence was significantly more important. Such results allowed the authors to
462 suggest that at Son Fornés pine trunks would have been used as constructive material (timber
463 for beams), while in Ses Païsses Aleppo pine charcoal fragments would mainly represent the
464 residues of the use of branches as firewood during the occupation of the building before the
465 final abandonment after the fire event.

466

467 Charcoal-pith distance has been measured on charcoal fragments from historical charcoal kilns
468 in order to interrogate forest resources management and the exploitation of woody vegetation
469 to produce energy sources. In this sense, Paradis-Grenouillet et al. (2015) identified the
470 continuous sustainable exploitation of *Fagus sylvatica* forests at Mont Lozère (France) during
471 four hundred years (11th to 15th centuries AD), based on beech coppicing practices by the
472 Medieval charcoal burners in relation to the metallurgical industry.

473

474 Finally, charcoal-pith distance has been measured on charcoal fragments associated with tree-
475 ring width and heartwood/sapwood (anthraco-typology) in four Neolithic sites located in
476 northern France (Houplin-Ancoisne in Deûle's Valley) and Alpine arc (Chalain 4 and Chalain
477 21 on Lake Chalain, Jura, France) (Coubray and Dufraisse, in press). These tools were
478 combined with the biological and ecological traits of the woody taxa identified for a systemic
479 approach to forest space. Two forest management systems are thus detected. The sites on Lake
480 Chalain are characterized by the exploitation of oak branches, probably from the hinterland,
481 and ash tree shoots from fragmentary woodland areas. In the Deûle Valley, it is the crown of
482 trees, such as ash and alder, which were exploited, whereas oak came mainly from the felling
483 of large trees. These data are integrated coherently into the paleoeconomic syntheses proposed
484 for these sites, namely, in a mountain context, semi-permanent habitats associated with a

485 shifting agriculture system in the forest where deer hunting played a predominant role, and in
486 the valley bottom a system of permanent habitats, structured within a densely occupied territory
487 where the share of livestock was dominant.

488

489 **Conclusion and perspectives**

490 The estimation of missing radius (CR, this is the charcoal-pith distance) by using the
491 trigonometric method, and the constitution of a reference dataset composed of 7 taxa allow
492 moving forward in the establishment of a reliable and less time-consuming PLT. This study
493 allows establishing a predictive model and estimating the missing radius and its interval of
494 confidence. This PLT, thus, allows a rapid and reliable measurement of the charcoal-pith
495 distance and, subsequently, an estimation of the original diameter up to 20 cm. Beyond this
496 diameter size, the margins of error detected increase considerably due to the insertion of new
497 rays during the growing of the tree and the creation of new rings.

498 In this sense, this study shows that carbonization is also a factor to be taken into account to
499 obtain reliable diameter estimations. In order to solve this, this experimental dataset allows
500 establishing correction factors of the wood shrinkage during carbonization to be applied to the
501 CR values obtained with the trigonometric semi-automatic PLT.

502 However, the access to specific equipment (multizoom microscope combined with a software
503 image analysis) is not always possible due to logistic reasons. We are therefore creating a
504 printed calibrated target based on the trigonometric principle; this means without taking into
505 account the tree-ring curvature but based on the angle and the distance between ligneous rays.
506 The target will be made freely available online (<https://dendrac.mnhn.fr/spip.php?article239>)
507 and can be printed out on different supports (rigid/soft). This target is ready to use under a
508 binocular stereomicroscope as a PLT to easily estimate a class of charcoal-pith distance (and
509 not a strict value) on charcoal fragments big enough.

510

511 **Acknowledgements**

512 The authors thank the Agence Nationale de la Recherche (ANR JCJC 200101 DENDRAC, dir.
513 A. Dufraisse) for financing this study. M.S. Garcia-Martinez's work was financed by the
514 Fundación Séneca of the Region of Murcia (Spain). The work of Ll. Picornell-Gelabert have
515 been done thanks to a Juan de la Cierva-Incorporación postdoctoral fellowship of the Spanish
516 Ministerio de Economía y Competitividad (IJCI-2015-24550). We also thank anonymous
517 referee for their comments.

518

519

520 **References**

- 521 Akaike, H., 1973. Information Theory and an Extension of the Maximum Likelihood Principle.
522 In: Petrov, B. N., & Csaki, F. (Eds.), Proceedings of the 2nd International Symposium on
523 Information Theory. Akademiai Kiado, Budapest, pp. 267-281
524
- 525 Applequist, M. B., B. 1958. A Simple pith locator for use with off-Center increment cores.
526 Journal of Forestry 56 (3), 141.
527
- 528 Chrzavzez, J., 2006. Collecte du bois de feu et paléoenvironnements au Paléolithique. Apport
529 méthodologique et étude de cas: la grotte de Fumane dans les Pré-Alpes Italiennes. Mémoire
530 de Master II, Université Paris I, (unpublished).
531
- 532 Coubray S., Dufraisse A. (2019) - De l'arbre à la forêt domestiquée : pratiques de gestion et
533 systèmes agroforestiers. Application de l'anthraco-typologie sur des sites néolithiques du Nord
534 de la France et du pourtour de l'arc alpin, in C. Montoya, J.-P. Fagnart et J.-L. Lochet
535 (dir.), *Préhistoire de l'Europe du Nord-Ouest. Mobilités, climats et identités culturelles*, actes
536 du 27^e congrès préhistorique de France (Amiens, 30 mai-4 juin 2016), vol. 3, Paris, Société
537 préhistorique française, p. 139-159.
538
- 539 Deleuze, C., Monreau, F., Renaud, J.P., Vivien, Y., Rivoire, M., Santenoise, Ph., Longuetaud,
540 F., Mothe, F., Hervé, J.C., Vallet, P., 2014. Estimer le volume total d'un arbre, quelles que
541 soient l'essence, la taille, la sylviculture, la station. RDV Techniques 44, ONF, pp. 22-32.
542
- 543 Dufraisse, A., 2005. Economie du bois de feu et sociétés néolithiques. Analyses
544 anthracologiques appliquées aux sites d'ambiance humide des lacs de Chalain et Clairvaux
545 (France, Jura). Gallia Préhistoire, 47, 187-233.
546
- 547 Dufraisse, A., Pétrequin, A. M., Pétrequin, P., 2007. La gestion du bois de feu : un indicateur
548 des contextes socio-écologiques. Approche ethnoarchéologique dans les Hautes Terres de
549 Papua (Nouvelle-Guinée indonésienne). In: Besse, M. (Ed.), Sociétés néolithiques. Des faits
550 archéologiques aux fonctionnements socio-économiques. Actes du 27^e colloque interrégional
551 sur le Néolithique (Neuchâtel, octobre 2005). Cahiers d'archéologie romande, Lausanne, vol.
552 108, pp. 115-126
553
- 554 Dufraisse, A., Garcia-Martinez, M.S., 2011. Mesurer les diamètres du bois de feu en
555 anthracologie. Outils dendrométriques et interprétation des données. Anthropobotanica 2, 1-18.
556
- 557 Dufraisse, A., Coubray, S., Nocus, N., Lemoine, M., Dupouey, J.-L., Marguerie, D., 2018.
558 Anthraco-typology as a key approach to past firewood exploitation and woodland management
559 reconstructions. Dendrological reference dataset modelling with dendro-anthracological tools.
560 Quat. Int. 463 Part B, 232-249. <https://doi.org/10.1016/j.quaint.2017.03.065>
561
562
- 563 Garcia-Martinez, M.S., Dufraisse, A., 2012. Correction factors on archaeological wood
564 diameter estimation. In: Badal E., Carrion Y., Grau E., Macías M., Ntinou M. (Eds), Wood and
565 charcoal: evidence for human and natural history, Saguntum extra 13, pp. 283-290.
566
- 567 Gaudin, S., 1996. Dendrométrie des peuplements. BTSA Gestion Forestière, Besançon.
568

569 Lev-Yadun, S., Aloni, R., 1995. Differentiation of the ray system in woody plants. The
570 botanical review 61 (1), 45-84
571

572 Ludemann, T., Nelle, O. (Eds.), 2002. Die Wälder am Schauinsland und ihre Nutzung durche
573 Bergau und Köhlerei. Fortwissenschaftliche Versuchs- und Forschungsanstalt Baden-
574 Württemberg, Freiburg.
575

576 Lundström-Baudais, K., 1986. Etude paléoethnobotanique de la station III de Clairvaux. In:
577 Pétrequin, P. (Ed.), Les sites littoraux néolithiques de Clairvaux-les-Lacs (Jura). I.
578 Problématique générale, l'exemple de la station III. Maison des Sciences de l'Homme, Paris,
579 pp. 311-391.
580

581 Marguerie, D., Hunot, J.-Y., 2007. Charcoal analysis and dendrology: data from archaeological
582 sites in western France. J. Archaeol. Sci. 34 (9), 1417-1433.
583 <https://doi.org/10.1016/j.jas.2006.10.032>
584

585 Muggeo, V. M. R., 2008. Segmented: an R package to fit regression models with broken-line
586 relationships. R News 8 (1), 20-25.
587

588 Nocus, N., 2014. Forêts et Sociétés aux étages planitiaires et collinéens de l'Alsace du
589 Néolithique au haut Moyen Age : approche dendro-anthracologique. Thèse de doctorat,
590 Museum national d'histoire naturelle, Paris, (unpublished).
591

592 Paradis-Grenouillet, S., Dufraisse, A., Allee, P., 2013. Radius of curvature measurements and
593 wood diameter: a comparison of different image analysis techniques. In: Damblon, F. (Ed.), 4th
594 International Meeting of Anthracology in Brussels, BAR International Series 2486, pp. 173-
595 182.
596

597 Paradis-Grenouillet, S., Allée, Ph., Servera-Vives, G., Ploquin, A., 2015. Sustainable
598 management of metallurgical forest on Mont Lozère (France) during the Early Middle Ages.
599 Environ. Archaeol. 20(2), 168-183. <https://doi.org/10.1179/1749631414Y.0000000050>
600

601 Paradis-Grenouillet, S., Dufraisse, A., 2018. Deciduous oak/chestnut: Differential shrinkage of
602 wood during charcoalification? Preliminary experimental results and implications for wood
603 diameter study in anthracology. Quat. Int. 463, 258-267.
604 <https://doi.org/10.1016/j.quaint.2017.06.074>
605

606 Picornell-Gelabert Ll., Asouti E., Allué Martí E., 2011. The ethnoarchaeology of firewood
607 management in the Fang villages of Equatorial Guinea, central Africa: Implications for the
608 interpretation of wood fuel remains from archaeological sites. J. Anthropol. Archeol. 30, 375-
609 384. <https://doi.org/10.1016/j.jaa.2011.05.002>
610

611 Picornell-Gelabert, Ll., Dufraisse, A., 2018. Wood for Building: Woodland Exploitation for
612 Timber Procurement in the Prehistoric and Protohistoric Balearic Islands (Mallorca and
613 Menorca; Western Mediterranean). Environ. Archaeol.
614 <https://doi.org/10.1080/14614103.2018.1521086>
615

616 Plomion, C., Leprovost G., Stokes, A., 2001. Wood Formation in Trees. Plant Physiology 127,
617 1513-1523.
618

619 Rozas, V., 2003. Tree age estimates in *Fagus sylvatica* and *Quercus robur*: testing previous and
620 improved methods. *Plant Ecology* 167, 193–212.
621
622 Willerding, U., 1971. Methodische problem bei der Untersuchung und Auswertung von
623 Pflanzensunden und frugeschichtlichen Siedlung. *Nachrichten aus Niedersachsens*
624 *Urgeschichte* 40, 180-188.
625
626 Xue, Q., Sun, W., Fagerstedt, K., Guo, X., Dong, M., Wang, W., and Cao, H., 2018. Effects of
627 wood rays on the shrinkage of wood during the drying process. *BioRes.* 13 (3), 7086-7095.
628 DOI: 10.15376/biores.13.3.7086-7095
629
630 Zapata Peña, L., Pena-Chocarro L., Ibanez Estevez J.J., Gonzalez Urquijo J.E., 2003.
631 Ethnoarchaeology in the Moroccan Jebala (Western Rif): wood, dung and fuel. In: Neumann,
632 K., Butler, A., Kahlheber, S. (Eds.), *Food, fuel and fields: progress in African archaeobotany.*
633 *Heinrich-Barth-Institut, Köln, Africa Praehistorica* 15, pp. 163-175.
634
635

636

637

638

Supplementary material 1:

We know from figure 2a that the relative error of the reconstructed diameters is really high for small angles. We tried to find a quantitative justification to set a lower limit under which the method should not be used because of too important errors.

Our first try was to identify outliers from the RE distribution as being outside 1.5 times the interquartile range above the upper quartile and below the lower quartile. The range of “normal data” was then [-0.825, 0.815]. We would then select only the data which angles are higher to the last observation being consider as outlier.

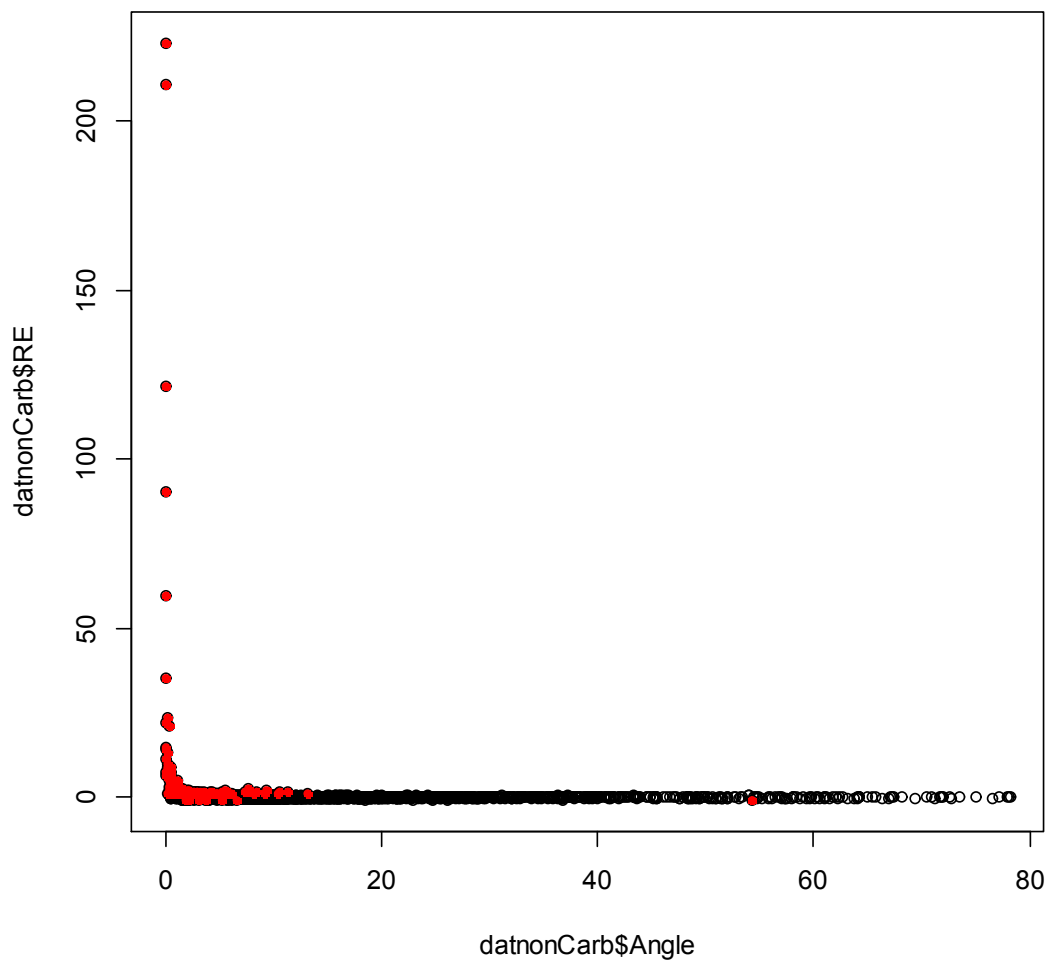


Figure SM1.1. Scatter plot of the relative errors of diameters estimations and angles. Red dots indicated data which are outside 1.5 times the interquartile range above the upper quartile and below the lower quartile { -0.825, 0.815}.

Unfortunately, an outlier appeared at an angle of 54.28 with an RE negative which was not what we expected to remove. Even by ignoring this point, the next limit was at 13.2 and we knew that linear

regression was quite good even for smaller angles. We then tried to include values inside a range of 99% around the median.

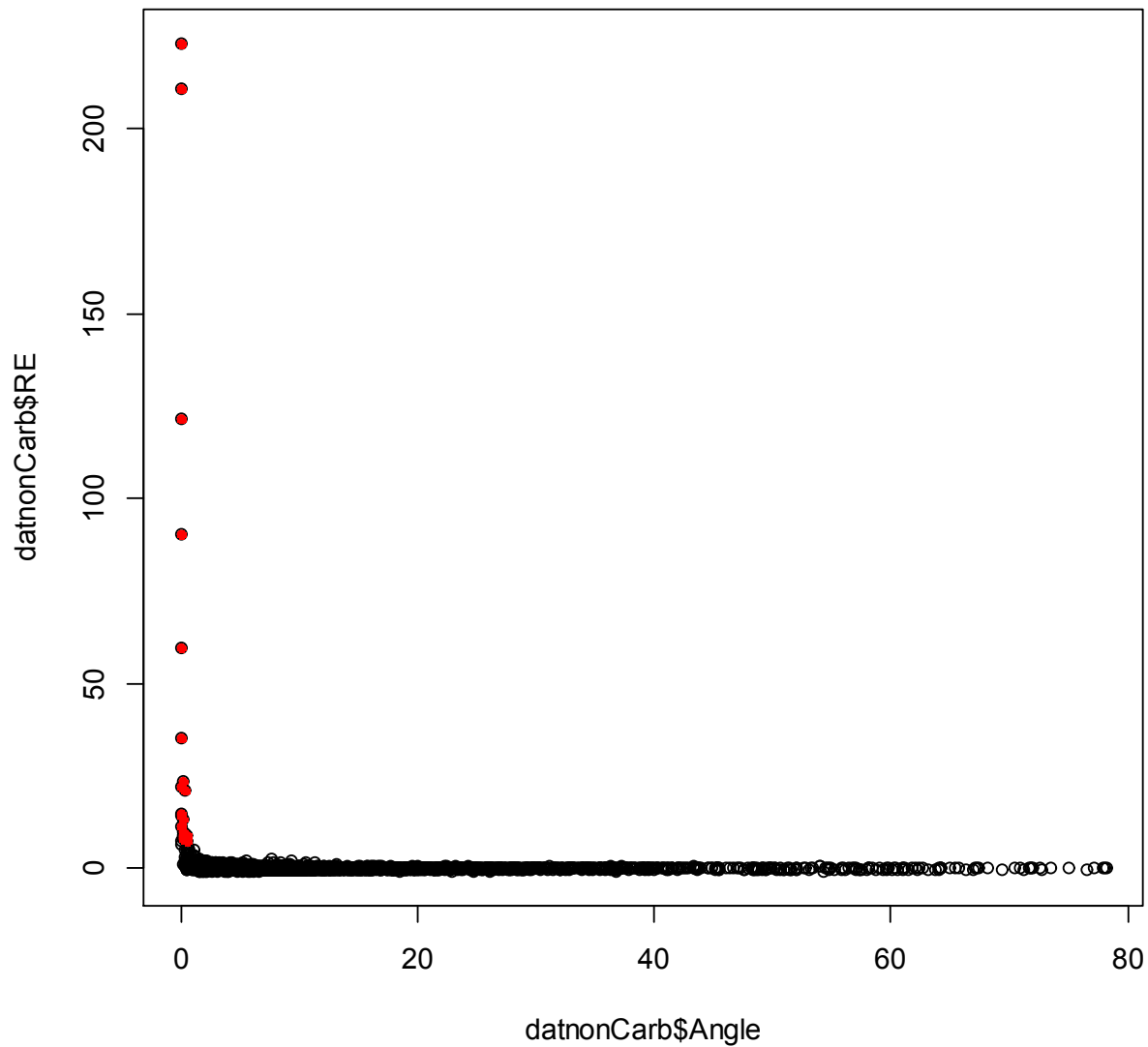


Figure SM1.2. Scatter plot of the relative errors of diameters estimations and angles. Red dots indicated data which are outside the 0.99 quantiles range $[-0.99000, 7.50295]$.

This time too many observations were kept and would have biased models very much at small angles. We finally considered that looking for outliers had some subjectivity in the quantile we would have selected to recognize the lower angle limit.

We then switched to Cook's distances (Cook & Weisberg, 1980) to identify points that would influence the regression too much in comparison to the others. The usual limit is 4 times the mean of the cook's distances of all the observations. This operation identifies four observations that are outside the limit (Fig. SM1.3).

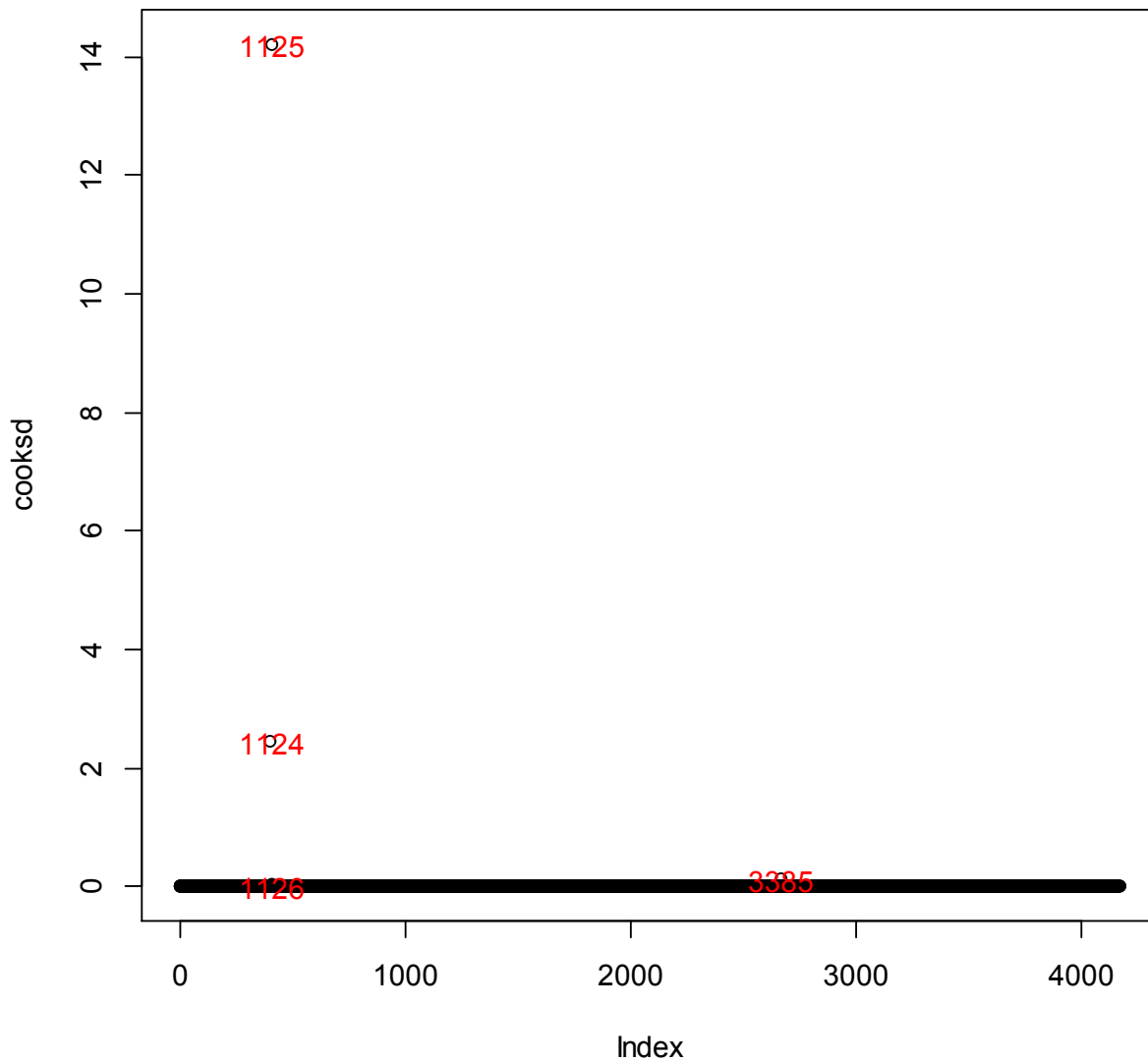


Figure SM1.3. Cook's distance of every point from the regression $RR = a * CR + b$.

We thus still have an important bias at small angles. We decided to try an iterative procedure by using a loop on the previous procedure and to run it until no points were outside the range. 46 runs were computed until it stabilized leaving only 983 points over the 4164 from the original dataset. This

reduction of the dataset would have too much weakens the study and the regressions would be artificially good.

We finally decided to compute moving average and dispersion intervals to recognize the point where the variability was reasonably small and the successive means centered on 0 (Fig.SM1.4, SM1.5). These two conditions are necessary to both have a good precision and resolution in our models. The value of 2 degrees appeared as the good balance between these properties and the number of points considered to build the models. We hope to find a more robust procedure in the future.

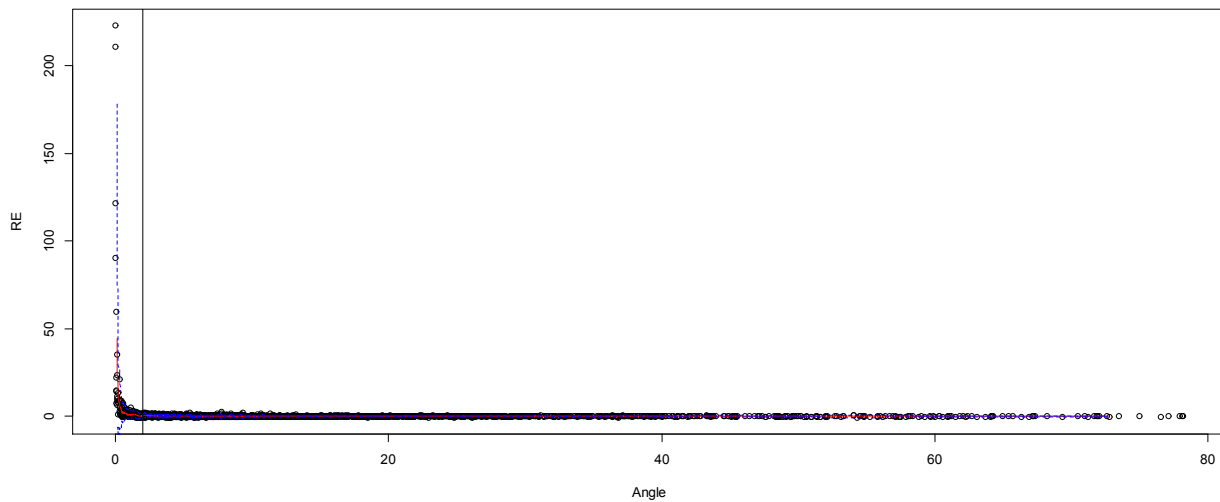


Figure SM1.4. Scatterplot of the Relative Errors and angles. Red line represents the moving average and blue dashed lines the moving average ± 2 standard deviations. Windows of 20 consecutive points. The vertical bars is angle = 2.

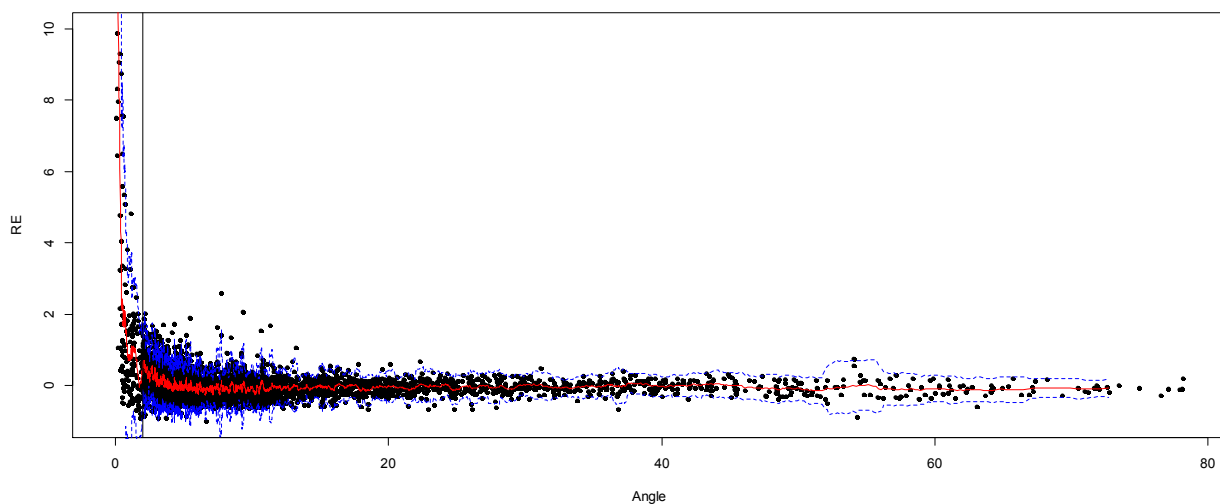


Figure SM1.5. Idem as fig.SM3.4 but limits of the y axis set to $\{-1, 10\}$.

Script:

```
# a common way to identify outliers is to consider as an outlier a value which is
# outside 1.5 times the interquartile range above the upper quartile and below the
# lower quartile.
# in our example lets check the variability of RE
qu<-quantile(datnonCarb$RE)
# so the range is
rangeQ<-c(qu[2]-(1.5*(qu[4]-qu[2])),qu[4]+(1.5*(qu[4]-qu[2])))
# we can remove lines which RE is outside [-0.825 , 0.815]
datnonCarbNoOut<-datnonCarb[datnonCarb$RE<rangeQ[2]&datnonCarb$RE>rangeQ[1],]
datnonCarbOut<-datnonCarb[datnonCarb$RE>rangeQ[2]|datnonCarb$RE<rangeQ[1],]
# check graphically
plot3d(datnonCarbNoOut$Distance,datnonCarbNoOut$RE,datnonCarbNoOut$Angle)
# which angles are related to these outliers
angleIn<-datnonCarb$Angle[datnonCarb$RE<rangeQ[2]&datnonCarb$RE>rangeQ[1]]
angleOut<-datnonCarb$Angle[datnonCarb$RE>rangeQ[2]|datnonCarb$RE<rangeQ[1]]
hist(angleOut)
hist(angleIn)
# many good RE are for small angles (~1400 for {0,5})
plot(datnonCarb$Angle,datnonCarb$RE)
points(datnonCarbOut$Angle,datnonCarbOut$RE, pch= 20,col="red")
# lets say now we want 99%
rangeQ<-quantile(datnonCarb$RE, probs = c(0,0.995))
datnonCarbNoOut<-datnonCarb[datnonCarb$RE<rangeQ[2]&datnonCarb$RE>rangeQ[1],]
datnonCarbOut<-datnonCarb[datnonCarb$RE>rangeQ[2]|datnonCarb$RE<rangeQ[1],]
plot(datnonCarb$Angle,datnonCarb$RE)
points(datnonCarbOut$Angle,datnonCarbOut$RE, pch= 20,col="red")
abline(v=2)
plot(datnonCarb$Angle,datnonCarb$RC)
points(datnonCarbOut$Angle,datnonCarbOut$RC, pch= 20,col="red")
## test avec cooks distances
mod <- lm(RR~Rctrigo, data=datnonCarb)
cooksds <- cooks.distance(mod)
plot(cooksds)
abline(h = 4*mean(cooksds, na.rm=T), col="red") # add cutoff line
text(x=1:length(cooksds)+1, y=cooksds, labels=ifelse(cooksds>4*mean(cooksds, na.rm=T),names(cooksds),""), col="red") # add
labels

datnonCarbCD<-datnonCarb[cooksds<4*mean(cooksds, na.rm=T),]
plot(RR~Rctrigo, data=datnonCarbCD)
# test loop cooks distance
isCD<-0
datnonCarbCD<-datnonCarb
count<-0
while (isCD!=1) {
  mod <- lm(RR~Rctrigo, data=datnonCarbCD)
  cooksds <- cooks.distance(mod)
  datnonCarbCD<-datnonCarbCD[cooksds<4*mean(cooksds, na.rm=T),]
  if(all(cooksds<4*mean(cooksds, na.rm=T))) {isCD<-1}
  plot(RR~Rctrigo, data=datnonCarbCD)
  count<-count+1
}
plot(RR~Rctrigo, data=datnonCarb)

## moving average on RE / Angle
width<-10
meansRE<-running(datnonCarb$RE[order(datnonCarb$Angle)],fun=mean,width=width,by=1)
```

```
meansAngle<-running(datnonCarb$Angle[order(datnonCarb$Angle)],fun=mean,width=width,by=1)
sdRE<-running(datnonCarb$RE[order(datnonCarb$Angle)],fun=sd,width=width,by=1)
plot(RE~Angle, data=datnonCarb),ylim=c(-1,10),pch=20)
lines(meansAngle,meansRE,col="red")
lines(meansAngle,meansRE-2*sdRE,col="blue",lty=2)
lines(meansAngle,meansRE+2*sdRE,col="blue",lty=2)
abline(v=2)
```

Additional references.

Cook, R. D. and Weisberg, S. (1982). *Residuals and Influence in Regression*. London: Chapman and Hall.

Legend

Table 1 – Number of measurements on perfect target performed with each PLT (manual and semi-automatic)

Table 2 – Number of measurements taken for each taxon. The reference number of the wood slices corresponds to that given for the dendro-anthracological reference collection, available to researchers (UMR 7209, Paris)

Table 3. Akaike Criterion Information (AIC) for the three models tested and R^2 of the best one for each taxon. reg: classic regression, wreg: weighted regression, swreg: segmented weighted regression. Values in bold represents the lowest AIC (the best model) corresponding for all taxa to swreg.

Table 4. Details of the swreg model for all taxa. The first slopes (lowest CR) are very similar between taxa. Notable differences are the breakpoints. Bold values indicate p-values lower than 0.05. P-values for breakpoints and slope 2 are not currently available; we use std.error to estimate the confidence in the results. The swreg model indicates significant differences between taxa regarding the breakpoints.

Table 5. Estimations, standard errors of the parameters and R^2 of the swregCarb model for *Pinus halepensis* (A) and *Fagus sylvatica* (B).

Figure 1: Kernel density of the relative errors (RE) measured on perfect targets. Comparison of manual and semi-automatic PLTs.

Figure 2: Biplots of angles between ligneous rays and relative errors (RE). A: representation of all the data, the vertical bar corresponds to an angle of 2° that is the threshold recommended in this paper. B: Boxplot of the data from which angles inferior to 2° have been removed and organized into classes.

Figure 3 – Scatter plot of the real radii (RR) over the calculated radii (CR), each panel corresponds to a taxon (fresh wood).

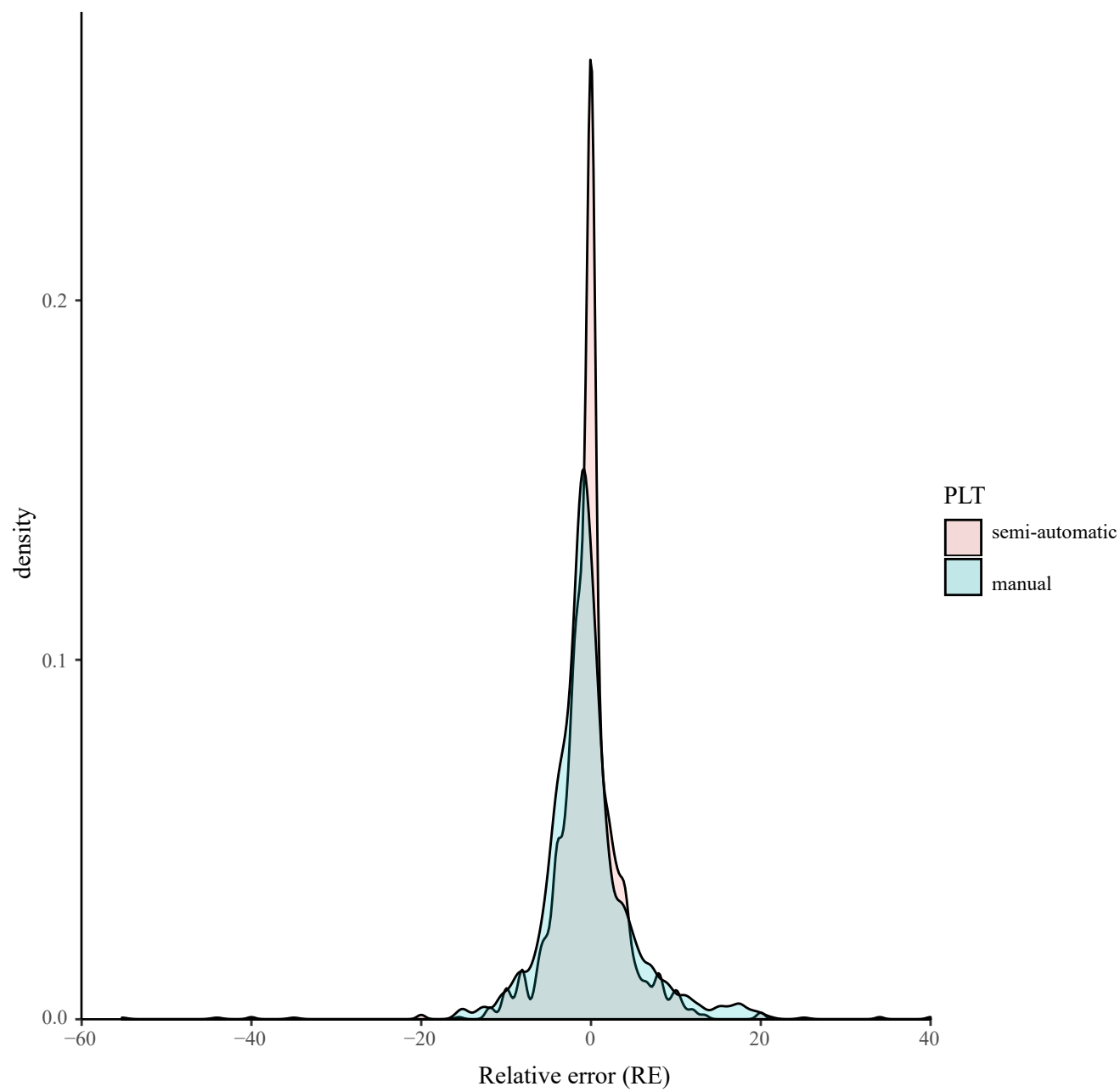
Figure 4 – Fitted lines corresponding to the swreg model for all taxa. The solid lines represent the estimation, the dashed lines represent the 0.95 prediction interval, and horizontal bars represent the 0.95 confidence interval around the estimation of the breakpoints represented by circles

Figure 5_ Fitted lines corresponding to the swregCarb model for *Pinus halepensis* and *Fagus sylvatica* whether or not carbonized. The solid lines represent the estimation and the dashed lines represent the 0.95 prediction interval.

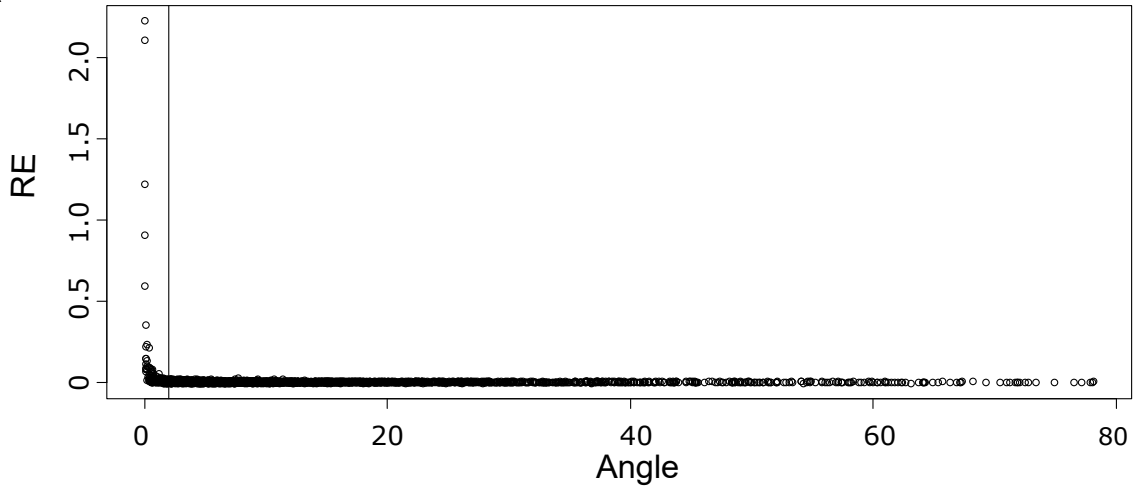
Figure 6 -a- Fresh wood of *Quercus petraea*, without tension wood. All the wood rays converge to the pith. b- Fresh wood of *Quercus petraea*, with tension wood. The direction of the rays changes to adapt to the new morphology of the wood.

SM 1 - the different statistical methods tried in order to provide the user a practical minimum angle

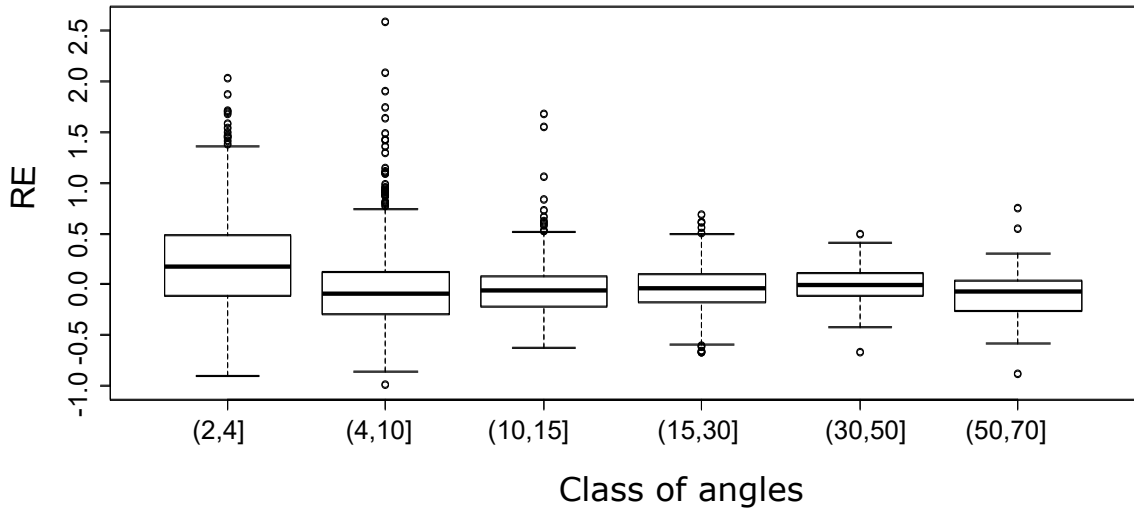
SM 2 – Boxplot of the relative errors (RE) on perfect targets depending on the distances between rays. A: Boxplot of all the data B: Boxplot of the data from which angles inferior to 2° have been removed.

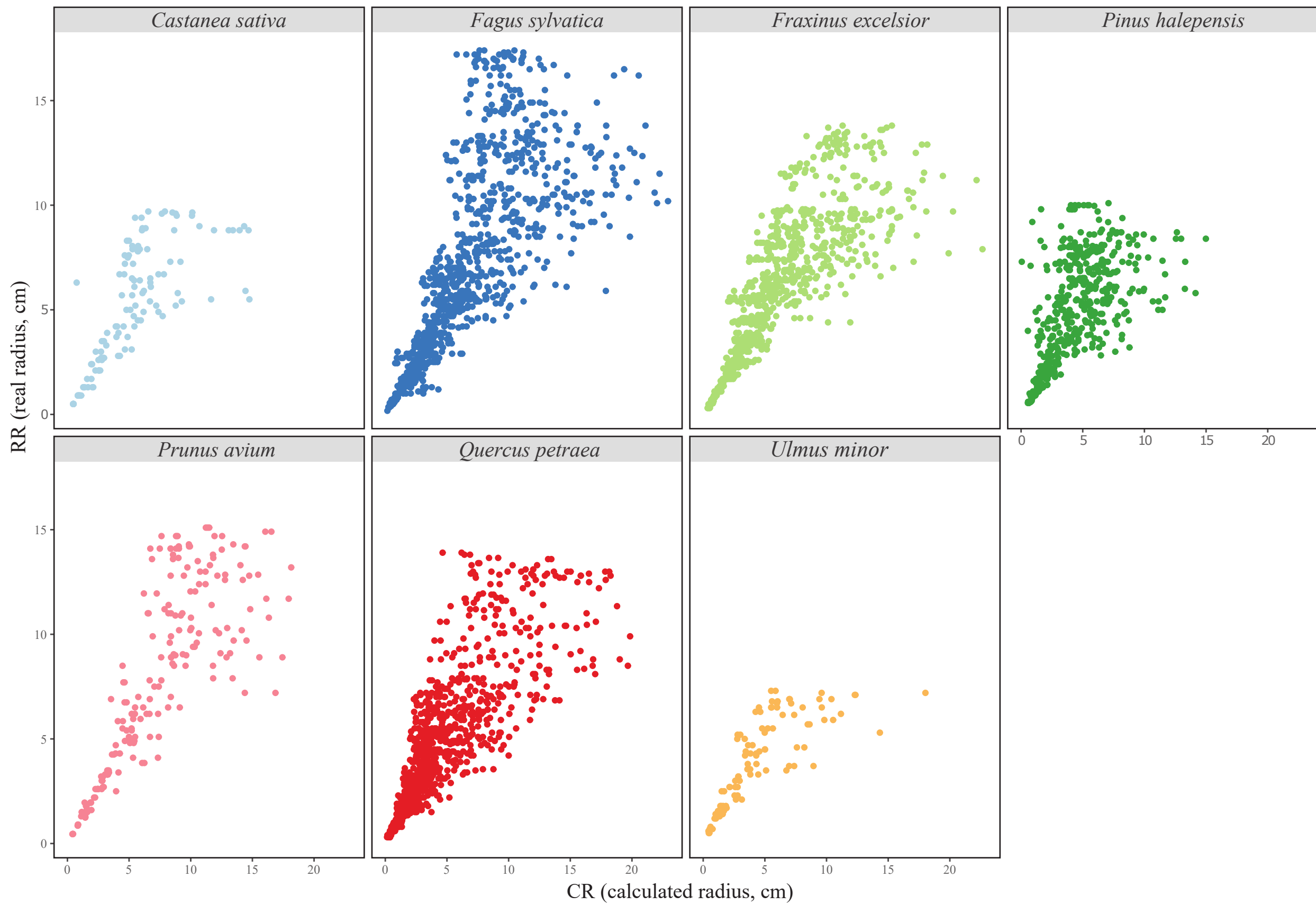


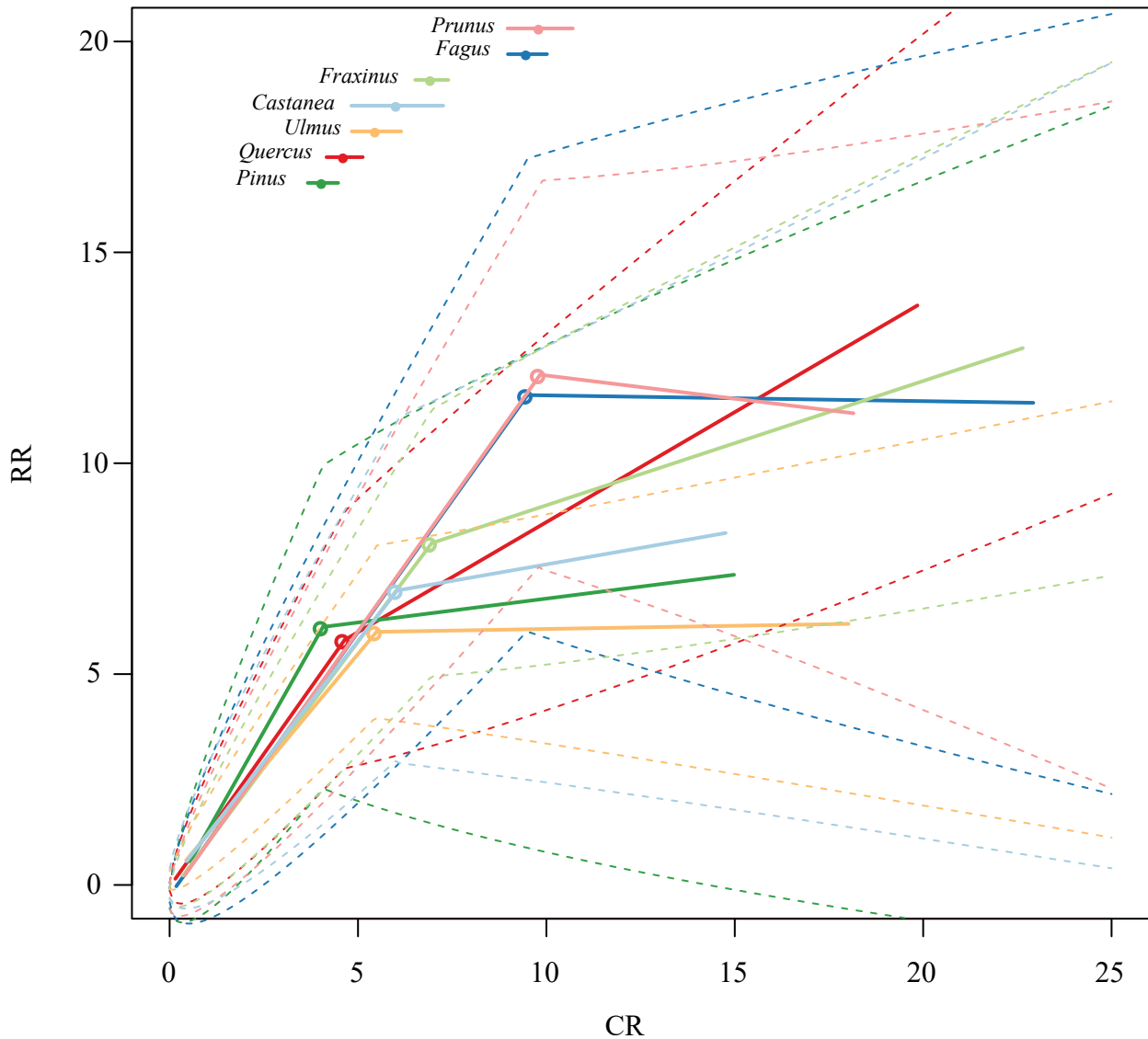
A



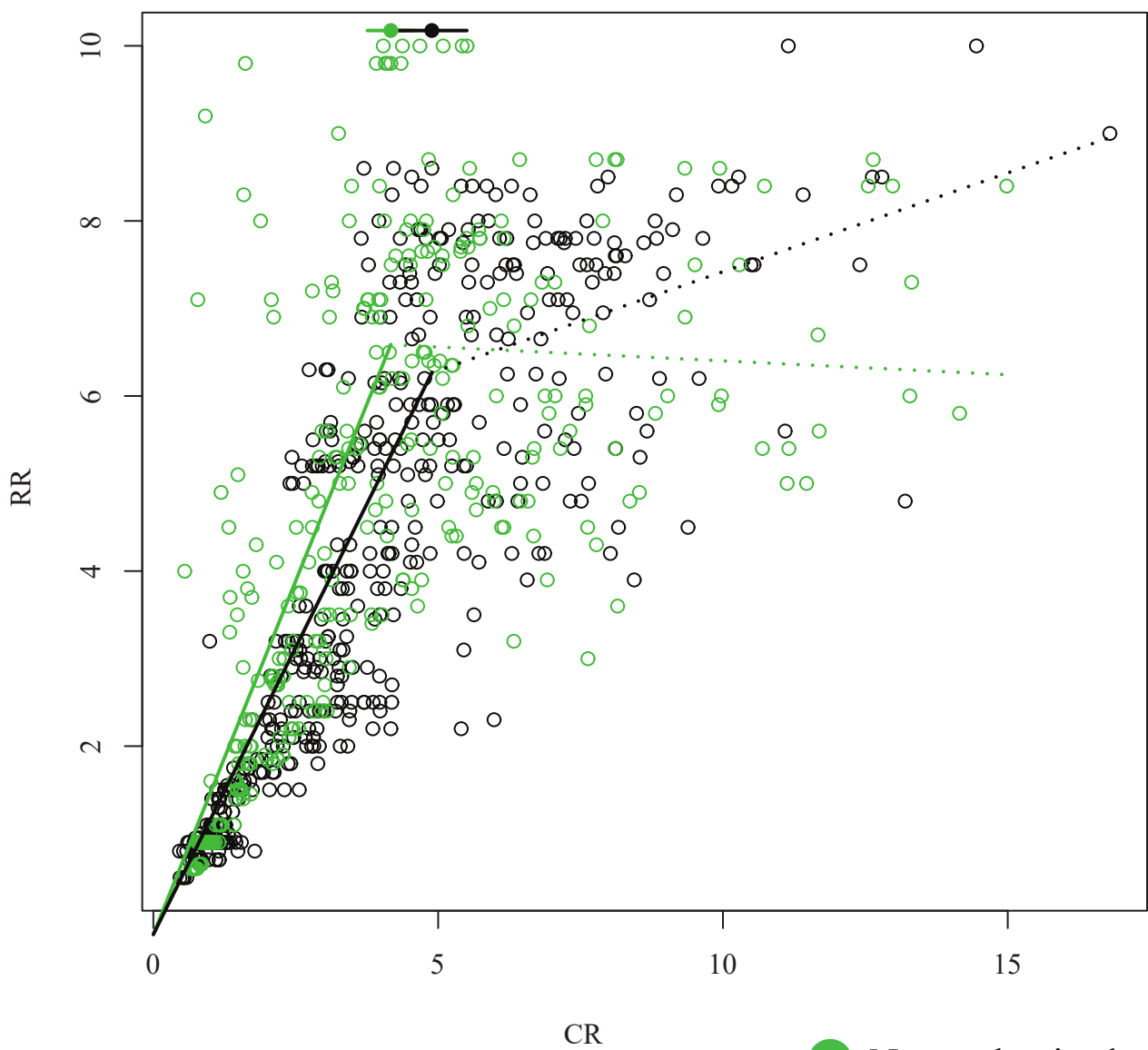
B





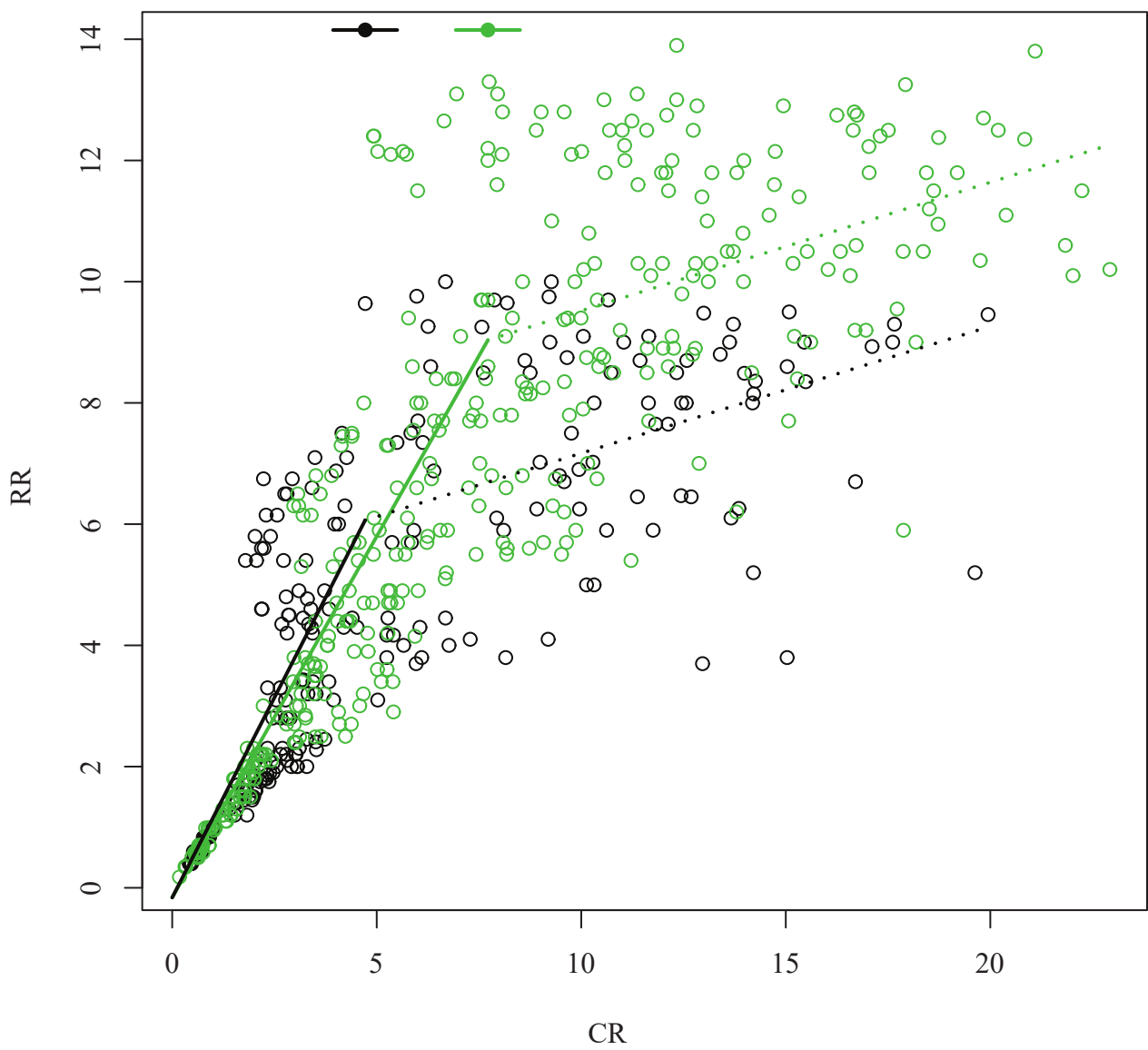


Pinus halepensis



- Non carbonized
- Carbonized

Fagus sylvatica



Author statement

Alexa Dufraisse : Conceptualization, Methodology, Archaeological data curation
, Writing- Original draft preparation, Supervision

Jérémie Bardin : Statistical treatment and modelisation

Llorenç Picornell-Gelabert : Archaeological data curation

Sylvie Coubray : Archaeological data curation

Maria Soledad Garcia-Martinez : modern reference data curation

Michel Lemoine : technical supervision

Sílvia Vila Moreiras : modern reference data curation